Universal Behavior of Two-Dimensional ^{3}He at Low Temperatures

V.R. Shaginyan,[1,2,*] A.Z. Msezane,[2] K.G. Popov,[3] and V.A. Stephanovich[4,†]

[1] *Petersburg Nuclear Physics Institute, RAS, Gatchina, 188300, Russia*
[2] *CTSPS, Clark Atlanta University, Atlanta, Georgia 30314, USA*
[3] *Komi Science Center, Ural Division, RAS, 3a, Chernova street Syktyvkar, 167982, Russia*
[4] *Opole University, Institute of Mathematics and Informatics, Opole, 45-052, Poland*

On the example of two-dimensional (2D) ^{3}He we demonstrate that the main universal features of its experimental temperature T - density x phase diagram [see M. Neumann, J. Nyéki, J. Saunders, Science **317**, 1356 (2007)] look like those in the heavy-fermion metals. Our comprehensive theoretical analysis of experimental situation in 2D ^{3}He allows us to propose a simple expression for effective mass $M^*(T,x)$, describing all diverse experimental facts in 2D ^{3}He in unified manner and demonstrating that the universal behavior of $M^*(T,x)$ coincides with that observed in HF metals.

PACS numbers: 72.15.Qm, 71.27.+a, 74.20.Fg, 74.25.Jb

One of the main purposes of condensed matter physics is to unveil the nature of the non-Fermi liquid (NFL) behavior in various strongly correlated Fermi-systems. These substances, such as high temperature superconductors, heavy fermion (HF) metals, 2D electron and ^{3}He systems are the objects of intensive studies leading to understanding of many-body effects and quantum phase transitions responsible for the NFL behavior. Heavy fermion metals provide important examples of strongly correlated Fermi-systems [1, 2]. In these compounds, being f-electron alloys, a lattice of f-electron spins couples to the itinerant electronic system by $s-f$ Kondo exchange interaction. The properties of such systems are now hotly debated as there is a common wisdom that they are related to zero temperature quantum fluctuations, suppressing quasiparticles and giving rise to a quantum critical point (QCP), where the systems transit to different magnetic ground states generating their specific NFL behavior [2, 3]. On the other hand, it was shown that the electronic system of HF metals demonstrates the universal low-temperature behavior irrespectively of their magnetic ground state [4]. Therefore it is of crucial importance to check whether this behavior can be observed in 2D Fermi systems. Fortunately, the recent measurements on 2D ^{3}He become available [5, 6]. Their results are extremely significant as they allow to check the presence of the universal behavior in the system formed by ^{3}He atoms which are essentially different from electrons. Namely, the neutral atoms of 2D ^{3}He are fermions with spin $S=1/2$ and they interact with each other by van-der-Waals forces with strong hardcore repulsion (due to electrostatic repulsion of protons) and a weakly attractive tail. The different character of interparticle interaction along with the fact, that a mass of He atom is 3 orders of magnitude larger then that of an electron, makes ^{3}He to have drastically different microscopic properties then that of 3D HF metals. Because of this difference nobody can be sure that the macroscopic physical properties of both above fermionic systems will be more or less similar to each other.

The bulk liquid ^{3}He is historically the first object, to which a Landau Fermi-liquid (LFL) theory had been applied [7]. This substance, being intrinsically isotropic Fermi-liquid with negligible spin-orbit interaction is an ideal object to test the LFL theory. Recently 2D ^{3}He sample has been fabricated and its thermodynamic properties have been thoroughly investigated [5, 6]. Our analysis of the experimental measurements has shown that the behavior of 2D ^{3}He is pretty similar to that of 3D HF compounds with various ground state magnetic properties. Because of van-der-Waals character of interparticle interaction, ^{3}He has a very important feature: the change of total density of ^{3}He film drives it towards QCP at which the quasiparticle effective mass M^* diverges [5, 8]. This peculiarity permits to plot the experimental temperature-density phase diagram, which in turn can be directly compared with theoretical predictions.

In this letter we show that despite of very different microscopic nature of 2D ^{3}He and 3D HF metals, their main universal features are the same, being dictated by a Landau quasiparticles paradigm. Namely, we demonstrate that the main universal features of ^{3}He experimental T - x phase diagram look like those in HF metals and can be well captured utilizing our notion of fermion condensation quantum phase transition (FCQPT) [9, 10, 11, 12, 13] based on the quasiparticles paradigm and thus deriving NFL properties of above systems from modified LFL theory. The modification is that in contrast to the Landau quasiparticle effective mass, the ^{3}He effective mass $M^*(T,x)$ becomes temperature and density dependent. We demonstrate that the universal behavior of $M^*(T,x)$ coincides with that observed in HF metals.

Let us consider HF liquid at $T=0$ characterized by the effective mass M^*. Upon applying the well-known equation, we can relate M^* to the bare electron mass M [7, 14] $M^*/M = 1/(1-N_0F^1(p_F,p_F)/3)$. Here N_0 is the density of states of a free electron gas, p_F is Fermi momentum, and $F^1(p_F,p_F)$ is the p-wave component of Landau interaction amplitude F. Since LFL theory im-

plies the number density in the form $x = p_F^3/3\pi^2$, we can rewrite the amplitude as $F^1(p_F, p_F) = F^1(x)$. When at some critical point $x = x_c$, $F^1(x)$ achieves certain threshold value, the denominator tends to zero so that the effective mass diverges at $T = 0$ and the system undergoes the fermion condensation quantum phase transition (FCQPT) [9, 10, 11, 12, 13]. The leading term of this divergence reads

$$\frac{M^*(x)}{M} = A + \frac{B}{1-z}, \; z = \frac{x}{x_c}, \tag{1}$$

where M is the bare mass, Eq. (1) is valid in both 3D and 2D cases, while the values of factors A and B depend on dimensionality and inter-particle interaction [13]. At $x > x_c$ the fermion condensation takes place. Here we confine ourselves to the case $x < x_c$.

When the system approaches FCQPT, the dependence $M^*(T, x)$ is governed by Landau equation [7, 13]

$$\frac{1}{M^*(T,x)} = \frac{1}{M} + \int \frac{\mathbf{p}_F \mathbf{p}}{p_F^3} F(\mathbf{p_F}, \mathbf{p}) \frac{\partial n(\mathbf{p}, T, x)}{\partial p} \frac{d\mathbf{p}}{(2\pi)^3}, \tag{2}$$

where $n(\mathbf{p}, T, x)$ is the distribution function of quasiparticles. The approximate solution of this equation is of the form [4]

$$\begin{aligned} \frac{M}{M^*(T)} &= \frac{M}{M^*(x)} + \beta f(0) \ln\{1 + \exp(-1/\beta)\} \\ &+ \lambda_1 \beta^2 + \lambda_2 \beta^4 + ..., \end{aligned} \tag{3}$$

where $\lambda_1 > 0$ and $\lambda_2 < 0$ are constants of order unity, $\beta = TM^*(T)/p_F^2$ and $f(0) \sim F^1(x_c)$. It follows from Eq. (3) that the effective mass $M^*(T)$ as a function of T and x reveals three different regimes at growing temperature. At the lowest temperatures we have LFL regime with $M^*(T) \simeq M^*(x) + aT^2$ with $a < 0$ since $\lambda_1 > 0$. This observation coincides with facts [5, 8]. The effective mass as a function of T decays up to a minimum and afterward grows, reaching its maximum $M_M^*(T, x)$ at some temperature $T_{\max}(x)$ with subsequent diminishing as $T^{-2/3}$ [13, 15]. Moreover, the closer is number density x to its threshold value x_c, the higher is the rate of the growth. The peak value M_M^* grows also, but the maximum temperature $T_{\max}$ lowers. Near this temperature the last "traces" of LFL regime disappear, manifesting themselves in the divergence of above low-temperature series and substantial growth of $M^*(x)$. The temperature region beginning near above minimum and continuing up to $T_{\max}(x)$ signifies the crossover between LFL regime with almost constant effective mass and NFL behavior, given by $T^{-2/3}$ dependence. Thus the $T_{\max}$ point can be regarded as crossover between LFL and NFL regimes. The latter regime sets up at $T \leq T_{\max}$, when $M^*(x) \to \infty$, giving rise to $T^{-2/3}$ effective mass decay [13, 15].

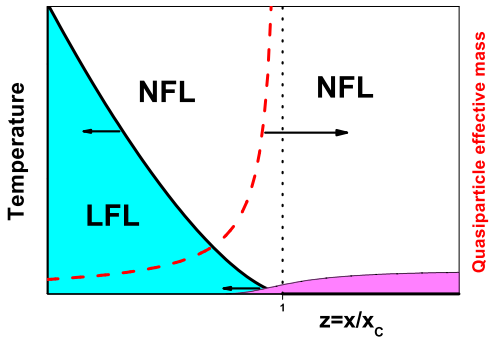

FIG. 1: The phase diagram of 2D ^{3}He. The part for $z < 1$ corresponds to HF behavior divided to the LFL and NFL parts by the line $T_{\max}(z) \propto (1-z)^{3/2}$, where $T_{\max}$ is the effective mass maximum temperature. The exponent $3/2 = 1.5$ coming from Eq. (5) is in good agreement with the experimental value 1.7 ± 0.1 [5]. The dependence $M^*(z) \propto (1-z)^{-1}$ is shown by the dashed line. The regime for $z \geq 1$ consists of LFL piece (the shadowed region, beginning in the intervening phase $z \leq 1$ [5], which is due to the substrate inhomogeneities, see text) and NFL regime at higher temperatures.

It turns out that $M^*(T, x)$ in the entire T and x range can be well approximated by a simple universal interpolating function similar to the case of the application of magnetic field [4, 13, 15]. The interpolation occurs between LFL ($M^* \propto T^2$) and NFL ($M^* \propto T^{-2/3}$) regimes thus describing the above crossover. Introducing the dimensionless variable $y = T/T_{\max}$, we obtain the desired expression

$$\frac{M^*(T,x)}{M_M^*} = \frac{M^*(y)}{M_M^*} = M_N^*(y) \approx \frac{M^*(x)}{M_M^*} \frac{1 + c_1 y^2}{1 + c_2 y^{8/3}}. \tag{4}$$

Here $M_N^*(y)$ is the normalized effective mass, c_1 and c_2 are parameters, obtained from the condition of best fit to experiment. Equation (1) shows that $M_M^* \propto 1/(1-z)$ and it follows from (3) that $M_M^* \propto T^{-2/3}$. As a result, we obtain

$$T_{\max} \propto (1-z)^{3/2}. \tag{5}$$

We note that obtained results are in agreement with numerical calculations [13, 15]. $M^*(T)$ can be measured in experiments on strongly correlated Fermi-systems. For example, $M^*(T) \propto C(T)/T \propto S(T)/T \propto M_0(T) \propto \chi(T)$ where $C(T)$ is the specific heat, $S(T)$ — entropy, $M_0(T)$ — magnetization and $\chi(T)$ — AC magnetic susceptibility. If the measurements are performed at fixed x then, as it follows from Eq. (4), the effective mass reaches the maximum at $T = T_{\max}$. Upon normalizing both $M^*(T)$ by its peak value at each x and the temperature by $T_{\max}$, we see from Eq. (4) that all the curves merge into single one demonstrating a scaling behavior.

In Fig. 1, we show the phase diagram of 2D ^{3}He in the variables T - z (see Eq. (1)). For the sake of comparison the plot of the effective mass versus z is shown by dashed

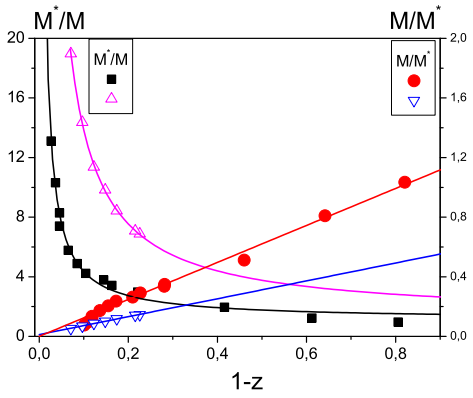

FIG. 2: The dependence of the effective mass $M^*(z)$ on dimensionless density $1-z = 1-x/x_c$. Experimental data from Ref. [8] are shown by circles and squares and those from Ref. [5] are shown by triangles. The effective mass is fitted as $M^*(z)/M \propto A + B/(1-z)$ (see Eq. (1)), while the reciprocal one as $M/M^*(z) \propto A_1 z$, where A, B and A_1 are constants.

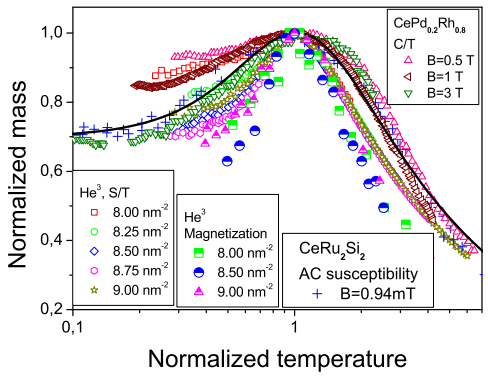

FIG. 3: The normalized effective mass M_N^* as a function of the normalized temperature $T/T_{\max}$ at densities shown in the left down corner. The behavior M_N^* is extracted from experimental data for $S(T)/T$ in 2D ^{3}He [6] and 3D HF compounds such as $CeRu_2Si_2$ and $CePd_{1-x}Rh_x$ [16, 17], fitted by the universal function (4).

line. The part of the diagram where $z < 1$ corresponds to HF behavior and consists of LFL and NFL parts, divided by the line $T_{\max}(z) \propto (1-z)^{3/2}$. We pay attention here, that our exponent $3/2 = 1.5$ is exact as compared to that from Ref. [5] 1.7 ± 0.1. The agreement between theoretical and experimental exponents suggests that our FCQPT scenario takes place both in 2D ^{3}He and in HF metals. The regime for $z > 1$ consists of low-temperature LFL piece, (shadowed region, beginning in the intervening phase $z \leq 1$ [5]) and NFL regime at higher temperatures. The former LFL piece is related to the peculiarities of substrate on which 2D ^{3}He film is placed. Namely, it is related to weak substrate heterogeneity (steps and edges on its surface) so that Landau quasiparticles, being localized (pinned) on it, give rise to LFL behavior [5, 6]. The competition between thermal and pinning energies

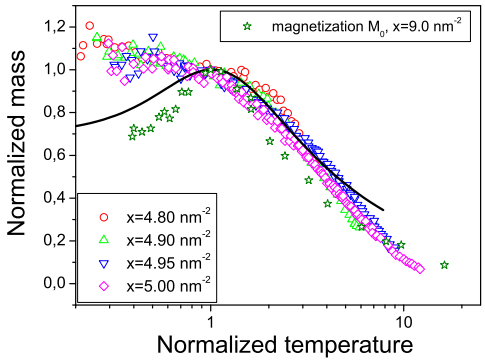

FIG. 4: The dependence $M_N^*(T/T_{\max})$ at densities shown in the left down corner. The behavior M_N^* is extracted from experimental data for $C(T)/T$ in 2D ^{3}He [8] and for the magnetization M_0 in 2D ^{3}He [5]. The solid curve shows the universal function, see the caption to Fig. 3.

returns the system back to FC state and hence restores the NFL behavior.

In Fig. 2, we report the experimental values of effective mass $M^*(z)$ obtained by the measurements on ^{3}He monolayer [8]. These measurements, in coincidence with those from Ref. [5], show the divergence of the effective mass at $x = x_c$. To show, that our FCQPT approach is able to describe the above data, we present the fit of $M^*(z)$ by the fractional expression $M^*(z)/M \propto A + B/(1-z)$ and the reciprocal effective mass by the linear fit $M/M^*(z) \propto A_1 z$. We note here, that the linear fit has been used to describe the experimental data for bilayer ^{3}He [5] and we use this function here for the sake of illustration. It is seen from Fig. 2 that the data in Ref. [5] (^{3}He bilayer) can be equally well approximated by both linear and fractional functions, while the data in Ref. [8] cannot. For instance, both fitting functions give for the critical density in bilayer $x_c \approx 9.8$ nm^{-2}, while for monolayer [8] these values are different - $x_c = 5.56$ for linear fit and $x_c = 5.15$ for fractional fit. It is seen from Fig. 2, that linear fit is unable to properly describe the experiment [8] at small $1-z$ (i.e. near $x = x_c$), while the fractional fit describes the experiment pretty good. This means that the more detailed measurements are necessary in the vicinity $x = x_c$.

Now we apply the universal dependence (4) to fit the experiment not only in 2D ^{3}He but in 3D HF metals as well. $M_N^*(y)$ extracted from the entropy measurements on the ^{3}He film [6] at different densities $x < x_c$ smaller then the critical point $x_c = 9.9 \pm 0.1$ nm^{-2} is reported in Fig. 3. In the same figure, the data extracted from heat capacity of ferromagnet $CePd_{0.2}Rh_{0.8}$ [16] and AC magnetic susceptibility of paramagnet $CeRu_2Si_2$ [17] are plotted for different magnetic fields. It is seen that the universal behavior of the effective mass given by Eq. (4) (solid curve in Fig. 3) is in accord with experimental facts. All substances are located at $x < x_c$, where the

system progressively disrupts its LFL behavior at elevated temperatures. In that case the control parameter, driving the system towards its critical point x_c is merely a number density x. It is seen that the behavior of the effective mass $M_N^*(y)$, extracted from $S(T)/T$ in 2D ^{3}He (the entropy $S(T)$ is reported in Fig. S8 A of Ref. [6]) looks very much like that in 3D HF compounds. As we shall see from Fig. 5, the amplitude and positions of the maxima of magnetization $M_0(T)$ and $S(T)/T$ in 2D ^{3}He follow nicely the interpolation formula (4). We conclude that Eq. (4) allows us to reduce a 4D function describing the effective mass to a function of a single variable. Indeed, the effective mass depends on magnetic field, temperature, number density and the composition so that all these parameters can be merged in the single variable by means of interpolating function like Eq. (4), see also Ref. [4].

The attempt to fit the available experimental data for $C(T)/T$ in ^{3}He [8] by the universal function $M_N^*(y)$ is reported below in Fig. 4. Here, the data extracted from heat capacity $C(T)/T$ for ^{3}He monolayer [8] and magnetization M_0 for bilayer [5], are reported. It is seen that the effective mass extracted from these thermodynamic quantities can be well described by the universal interpolation formula (4). We note the qualitative similarity between the double layer [5] and monolayer [8] of ^{3}He seen from Fig. 4.

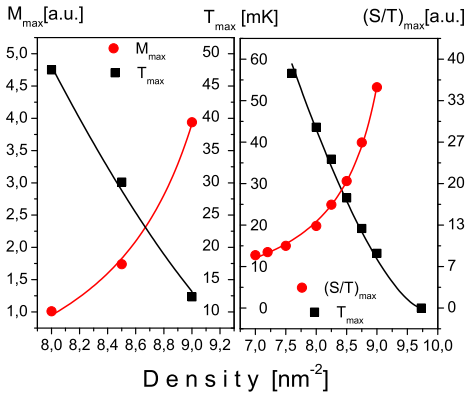

FIG. 5: Left panel, the peak temperatures $T_{\max}$ and the peak values $M_{\max}$ extracted from measurements of the magnetization M_0 in ^{3}He [5]. Right panel shows $T_{\max}$ and the peak values $(S/T)_{\max}$ extracted from measurements of $S(T)/T$ in ^{3}He [6]. We approximate $T_{\max} \propto (1-z)^{3/2}$ and $(S/T)_{\max} \propto M_{\max} \propto A/(1-z)$.

On the left panel of Fig. 5, we show the density dependence of $T_{\max}$, extracted from measurements of the magnetization $M_0(T)$ on ^{3}He bilayer [5]. The peak temperature is fitted by Eq. (5). At the same figure, we have also reported the maximal magnetization $M_{\max}$. It is seen that $M_{\max}$ is well described by the expression $M_{\max} \propto (S/T)_{\max} \propto (1-z)^{-1}$, see Eq. (1). The right panel of Fig. 5 reports the peak temperature $T_{\max}$ and the maximal entropy $(S/T)_{\max}$ versus the number density x. They are extracted from the measurements of $S(T)/T$ on ^{3}He bilayer [6]. The fact that both the left and right panels have the same behavior shows once more that there are indeed the quasiparticles, determining the thermodynamic behavior of 2D ^{3}He (and also 3D HF compounds [4]) near their QCP.

To conclude, we have described the diverse experimental facts related to temperature and number density dependencies of thermodynamic characteristics of 2D ^{3}He by the single universal function of one argument. The above universal behavior is also inherent to HF metals with different magnetic ground states. Also, for the first time, the amplitude and positions of the maxima of the magnetization $M_0(T)$ and the entropy $S(T)/T$ in 2D ^{3}He as the functions of density have been analyzed on Fig.5. We obtain the marvelous coincidence with experiment in the framework of our theory. Moreover, these data could be obtained for ^{3}He only and thus they were inaccessible for analysis in HF metals. This fact also shows the universality of our approach. Thus we have shown that bringing the experimental data collected on different strongly correlated Fermi-systems to the above form immediately reveals their universal scaling behavior.

This work was supported in part by the RFBR No. 08-02-00038, DOE and NSF No. DMR-0705328.

* Electronic address: vrshag@thd.pnpi.spb.ru
† Electronic address: stef@math.uni.opole.pl

[1] G.R. Stewart, Rev. Mod. Phys. **73**, 797 (2001).
[2] H.v. Löhneysen, A. Rosch, M. Vojta, P. Wölfle, Rev. Mod. Phys. **79**, 1015 (2007).
[3] P. Coleman and A.J. Schofield, Nature **433**, 226 (2005).
[4] V.R. Shaginyan, K.G. Popov, and V.A. Stephanovich, Europhys. Lett. **79**, 47001 (2007).
[5] M. Neumann, J. Nyéki, J. Saunders, Science **317**, 1356 (2007).
[6] Supporting online material for Ref. [5].
[7] L.D. Landau, Sov. Phys. JETP, **3**, 920 (1956).
[8] A. Casey, H. Patel, J. Nyéki, B. P. Cowan, and J. Saunders, Phys. Rev. Lett. **90**, 115301 (2003).
[9] V.A. Khodel and V.R. Shaginyan, JETP Lett, **51**, 553 (1990).
[10] V.A. Khodel, V.R. Shaginyan, and V.V. Khodel, Phys. Rep. **249**, 1 (1994).
[11] M. Ya. Amusia and V.R. Shaginyan, Phys. Rev. B **63**, 224507 (2001).
[12] G.E. Volovik, *in Quantum Analogues: From Phase Transitions to Black Holes and Cosmology*, eds. William G. Unruh and R. Schutzhold, Springer Lecture Notes in Physics **718**, pp. 31-73 (2007); cond-mat/0601372
[13] V.R. Shaginyan, M.Ya. Amusia, and K.G. Popov, Physics-Uspekhi, **50**, 563 (2007).
[14] M. Pfitzner and P. Wölfle, Phys. Rev. B **33**, 2003 (1986).
[15] J.W. Clark, V.A. Khodel, and M.V. Zverev Phys. Rev. B **71**, 012401 (2005).
[16] A.P. Pikul *et al.,* J. Phys. Condens. Matter **18**, L535

(2006).
[17] D. Takahashi *et al.,* Phys. Rev. B **67**, 180407(R) (2003).